Journal of Applied Electrochemistry **32**: 267–273, 2002.

Temperature dependence studies of a.c. impedance of lithium-ion cells

P. SURESH[1], A.K. SHUKLA[1] and N. MUNICHANDRAIAH[2]*
[1]*Solid State and Structural Chemistry Unit*
[2]*Department of Inorganic and Physical Chemistry, Indian Institute of Science, Bangalore, 560 012, India*
*(*author for correspondence, fax: +91 80 3600683, e-mail: muni@ipc.iisc.ernet.in)*

Received 5 September 2001; accepted in revised form 19 February 2002

Key words: a.c. impedance; kinetic parameters, lithium-ion cell, NLLS fit, temperature dependence

Abstract

The a.c. impedance behaviour of a commercial sealed Li-ion cell is studied in the temperature range −10 to 40 °C at various state-of-charge (SOC) values. The data comprise an inductive part in the frequency region of 100 kHz–100 Hz, and two capacitive parts in the frequency region of 100 Hz–10 mHz. The data are analysed using an equivalent circuit and a nonlinear least square fitting procedure, and the impedance parameters are evaluated. The inductance is found to be independent of temperature and SOC of the cell. The resistance corresponding to the high frequency semicircle of the Nyquist impedance plot, which is attributed to the surface film on the electrodes, shows a weak dependence on the SOC of the cell. On the other hand, it exhibits Arrhenius dependence on temperature. A value of 0.4 ± 0.05 eV is obtained for activation energy of charge-transport in the surface film. The resistance corresponding to the low frequency semicircle is due to the electron-transfer reactions, and exhibits a strong dependence on the SOC and also temperature. The data are analysed using the Butler–Volmer kinetic equation for activation controlled charge-transfer reaction, and the kinetic parameters, namely, the apparent exchange current, transfer coefficient and activation energy of the cell reaction are evaluated.

1. Introduction

Electrochemical impedance spectroscopy has been employed as a versatile experimental technique for non-destructive evaluation of several electrochemical parameters [1]. The a.c. impedance measurements of several battery systems have been reported and reviewed [2–4]. In recent years, investigations on research and development of the Li-ion battery have been in progress [5–7]. The operating voltage of a Li-ion cell is in the 3.0–4.2 V range with an energy density as high as 120 Wh kg^{-1} at ambient temperature.

As the Li-ion cell yields the highest energy density among existing rechargeable batteries, it is being evaluated for use in a variety of applications ranging from portable consumer electronic devices to space vehicles. Studies on performance behaviour of Li-ion cells at low temperatures have been of interest recently [8–11]. By measuring several electrical characteristics of Li-ion cells from three different manufacturers, it has been concluded by Nagasubramanian [8] that the electrical performance of these cells below 0 °C is poor. The poor performance has been attributed to an increase in interfacial resistance at subambient temperatures. Low temperature behaviour of Li-ion cells made of *meso*-carbon microbead (MCMB) anode and $LiCoO_2$ cathode has been studied by Lin et al. [9]. It has been suggested that the loss in delivered capacity of the MCMB-$LiCoO_2$ cell is due to increased resistance of the solid electrolyte interface, which results from deposition of metallic Li during low temperature charging. Electrolyte solutions of $LiPF_6$ and $LiAsF_6$ in solvents of ternary mixtures have been studied by Shiao et al. [10] with a view to enhance the low temperature performance of Li-ion cells. Irreversible capacity loss of graphite anode in several electrolytes has been studied by Smart et al. [11]. It is understood, to the best of the authors' knowledge, that a systematic study on the temperature dependence of a.c. impedance behaviour of Li-ion cells has not been reported.

In the present study, a.c. impedance data at different states-of-charge (SOC) of a commercial Li-ion cell in the temperature range −10 to 40 °C are measured. The data are analysed by means of an electrical equivalent circuit and a nonlinear least square (NLLS) fitting procedure. The impedance parameters, which show dependence on SOC and temperature, are used for evaluation of kinetic parameters of the Li-ion cell reaction.

2. Experimental details

Sealed Li-ion rechargeable cells (Samsung model BTL1030M) of 0.9 Ah nominal capacity at ambient

temperature were employed for the present study. The cell is intended for powering cellular phones (Samsung) and the cell-container forms a part of the body of the phone. The polymeric case of the cell and the mini-electronic circuit were disconnected. The electrical leads of the individual electrodes terminating on the sealed stainless steel container were directly connected to the measuring equipment. The electrical circuit employed for constant current charge/discharge cycling of the cell between the voltage limits of 3.0 and 4.2 V consisted of a regulated d.c. power source, a high resistance and an ammeter in series with the cell. The cell voltage was measured using a digital multimeter of high input impedance. A.c. impedance measurements of the Li-ion cell were carried out in the frequency range 100 kHz–10 mHz by an electrochemical impedance analyser (EG&G PARC model 6310). The cell was excited by an a.c. signal of 5 mV at open-circuit conditions. For measurements at a required SOC, the cell was discharged at $C/5$ rate to reach 3.0 V and then charged to the required SOC at the same rate at ambient temperature. For the purpose of experiments in the temperature range from -10 to 40 °C, a refrigerator cum heating instrument (Julabo model F 25) with ethylene glycol and water mixture as the thermal medium was employed. The cell was inserted into an insulated glass container. A thermal sensor (PT 100) mounted close to the cell allowed measurement of the temperature of the cell within ± 0.5 °C. At the required temperature, the cell was equilibrated for 3 h before measurements.

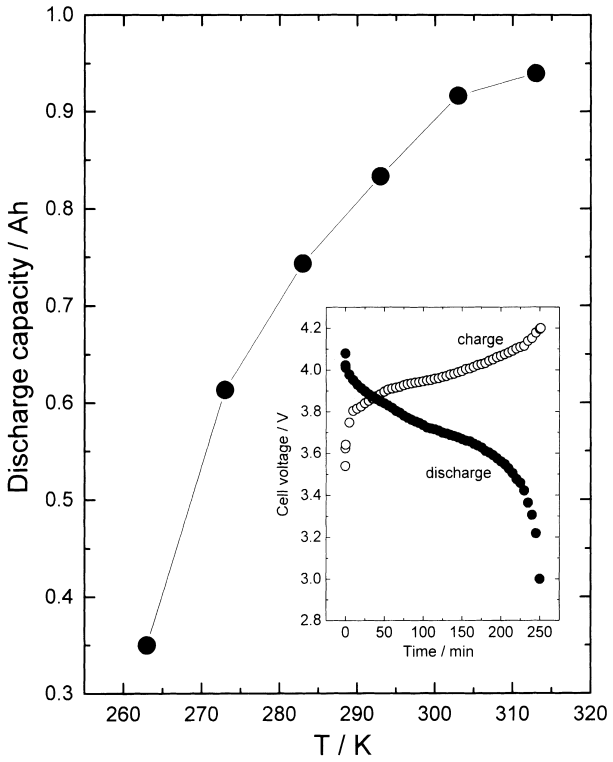

Fig. 1. Discharge capacity of the Li-ion cell against temperature (T). The charge/discharge curves typically at 20 °C are shown in the inset. Current 0.2 A.

3. Results and discussion

The negative and positive electrodes of a Li-ion cell are generally made of lithiated graphite and $LiCoO_2$, respectively, and the electrolyte is a Li salt dissolved in an aprotic solvent. The respective electrode-reactions are as given below [6]:

$$LiC \underset{\text{charge}}{\overset{\text{discharge}}{\rightleftharpoons}} Li_{1-x}C + xLi^+ + xe^- \quad E^\circ = -3.0\ \text{V} \qquad (1)$$

$$Li_{1-x}CoO_2 + xLi^+ + xe^- \underset{\text{charge}}{\overset{\text{discharge}}{\rightleftharpoons}} LiCoO_2 \quad E^\circ = 0.6\ \text{V} \qquad (2)$$

The overall cell reaction, therefore, is as given in Equation 3:

$$LiC + Li_{1-x}CoO_2 \underset{\text{charge}}{\overset{\text{discharge}}{\rightleftharpoons}} Li_{1-x}C + LiCoO_2$$
$$E^\circ_{\text{cell}} = 3.6\ \text{V} \qquad (3)$$

The variation of cell voltage during a charge–discharge cycle and the variation of discharge capacity with temperature are shown in Figure 1. The capacity of the Li-ion cell at ambient temperature is about 0.9 Ah, and it decreases to a value as low as 0.35 Ah at -10 °C. On the other hand, there is a marginal increase in capacity with increase of temperature up to 40 °C. The poor performance of the Li-ion cell at low temperatures is due to poor electrode kinetics, as discussed below on the basis of a.c. impedance data.

Impedance spectra in the Nyquist form of the Li-ion cell at SOC value of 0.5 and different temperatures are shown in Figure 2. At all temperatures and SOC values, the spectrum is characterized by an inductive region in the high frequency range, a small semicircle in the middle frequency range and a larger semicircle in the low frequency range. The size of the semicircle decreases with increase in temperature.

The impedance parameters were evaluated by fitting the data to an equivalent circuit using the NLLS fitting procedure due to Boukamp [12]. The equivalent circuit, which was found to fit the experimental impedance spectra satisfactorily, is shown in Figure 3. The circuit elements are explained as follows. The high frequency impedance data are inductive in nature (Figure 2). Therefore, the inductance (L) and the resistance (R_L) corresponding to the inductance data are taken in parallel. The element R_Ω represents the ohmic resistance of the cell, which includes the resistance of the electrolyte, separator, current collectors, electrical leads etc. The impedance spectrum (Figure 2) consisting of two semicircles is due to two pairs of parallel resistances and capacitances [13]. However, the semicircles are de-

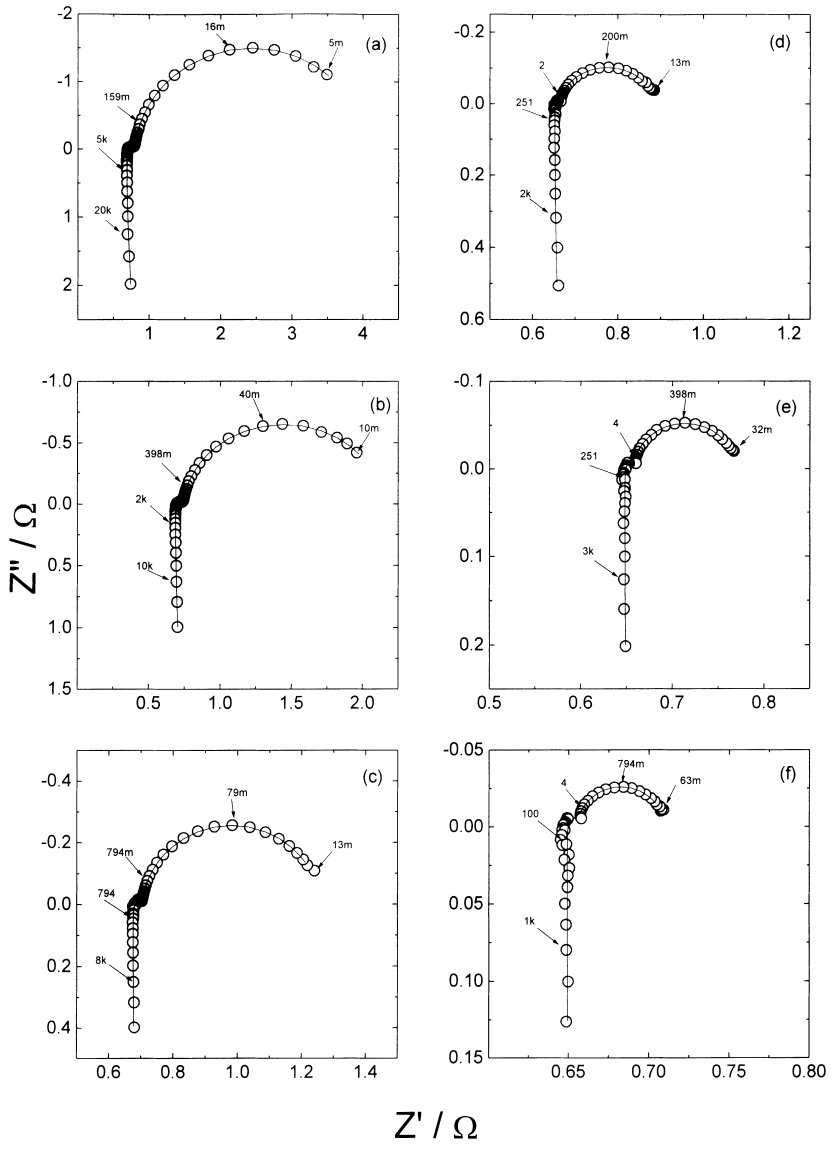

Fig. 2. Nyquist impedance spectra of the Li-ion cell at SOC ≈ 0.5 at different temperatures: (a) −10, (b) 0, (c) 10, (d) 20, (e) 30 and (f) 40 °C. Experimental data: symbols; simulated spectra from NLLS fit results: curves. Frequency values (Hz) are given for some data points.

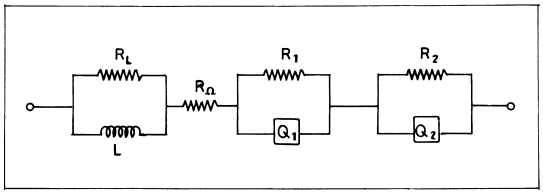

Fig. 3. Equivalent circuit used for NLLS-fitting of the experimental data of the Li-ion cell.

pressed with their centres falling below the real axis. Therefore, a constant phase element (CPE) is considered in place of a capacitance. Accordingly, R_1 and Q_1 are resistance and CPE, respectively, corresponding to the high frequency semicircle, and R_2 and Q_2 are resistance and CPE, respectively, corresponding to the low frequency semicircle. As discussed below R_1 and R_2, respectively, are the resistance of the surface film on the electrodes and the charge-transfer resistance of the cell reaction. Q_1 and Q_2, respectively, are constant phase elements corresponding to the surface film capacitance and double-layer capacitance. The CPE arises due to distribution of microscopic material properties [1], and in the admittance representation, the CPE is given as [12]

$$Q^* = Q_0(\mathrm{j}\omega)^n \tag{4}$$

where Q_0 is an adjustable parameter and $\omega = 2\pi f$, f being the a.c. frequency. For $n = 0$, CPE represents a resistance, $R\ (= Q_0^{-1})$; for $n = 1$, a capacitance, $C\ (=Q_0)$; for $n = 0.5$, a Warburg impedance, and for $n = -1$, an inductance, $L\ (=Q_0^{-1})$. The NLLS fitting proceeded through several iterations and the best-fit parameters were obtained. The chi-square value of the fit was lower than the 10^{-5}, and the correlation coefficients are >0.1 or <-0.1, thus, suggesting a good NLLS fit [14]. Furthermore, the simulated impedance spectrum gener-

Table 1. Impedance parameters of the Li-ion cell at SOC ≈ 0.5

Parameter	Temperature/K					
	263	*273*	*283*	*293*	*303*	*313*
R_L/Ω	69.640	53.660	47.660	48.660	49.670	46.190
$L/\mu H$	7.945	7.949	7.939	7.947	8.017	9.977
R_Ω/Ω	0.685	0.686	0.675	0.653	0.648	0.649
R_1/Ω	0.120	0.060	0.029	0.013	0.009	0.007
Q_1	0.521	0.539	0.668	0.618	0.947	0.959
n_1	0.569	0.631	0.705	0.956	1.000	1.000
R_2/Ω	3.253	1.398	0.556	0.221	0.113	0.053
Q_2	3.377	3.382	3.482	3.573	3.745	3.808
n_2	0.949	0.954	0.946	0.949	0.946	0.981

ated from the fit values of the parameters agrees well with the experimental spectrum, as shown in Figure 2. A similar fit procedure has enabled us to analyze the impedance parameters for identification of suitable parameters that show strong dependence on SOC of commercial Li-ion batteries [15] at ambient temperature. Typically at SOC ≈ 0.5, the values of impedance parameters of the Li-ion cell obtained at different temperatures are given in Table 1.

In general, battery systems are known to exhibit inductance behaviour in the high frequency range [4] due to the reversible storage of electrical energy [16] and to the geometrical nature of conductors and electrodes [17]. The value of the inductance obtained from fitting of the impedance of the lithium-ion cell at all SOC values in the temperature range between -10 and 40 °C, is about 8 μH, which is invariant with SOC and temperature. The invariance of L indicates that the origin of this parameter is geometrical and not electrochemical. This also suggests a possible coupling of stray inductance from cell leads and cables with the cell parameters [17]. Hence, L is not an appropriate parameter to study the dependence of both temperature and SOC.

The ohmic resistance of the Li-ion cell, R_Ω, includes contributions from the electrolyte, interelectrode separator, electrode materials, current collectors and cell terminals. Among these cell components, the electrolyte offers ionic resistance and the rest of the components electronic resistance. The net cell reaction (Equation 3) suggests that the concentration of the electrolyte remains unaltered with SOC and hence the electrolyte resistance is expected to be invariant with SOC. However, the ionic resistance of the electrolyte is expected to decrease with increase in temperature. An examination of the data of a recent study [10] suggests that the resistance of Li-ion battery electrolyte decreased by about 50% when the temperature was raised from -10 to 20 °C. A similar variation in R_Ω of the present study may be expected, if this parameter is due to the electrolyte resistance alone. On the contrary, the value of R_Ω is in the range 0.60–0.65 Ω, which is invariant with SOC and temperature (Table 1). While the electronic resistance of the electrode active materials may depend on SOC due to changes in their compositions, the resistance of the other passive components (current collectors, terminals etc.) is expected to be invariant with SOC. However, the electronic resistance is expected to increase with temperature. The near nonvariance of R_Ω with temperature suggests that the decreasing effect of electrolyte resistance is compensated by the increasing effect of the resistance due to the electronic conductors. The poor low temperature discharge capacity of the Li-ion cell (Figure 1), therefore, is not due to increase in ohmic resistance of the Li-ion cell.

Similarly to the data of the present study, a pair of capacitive semicircles of unequal dimensions has been reported in the literature [18–22] for Li-ion cells. The low frequency larger semicircle has been attributed to charge-transfer at the carbon anode and the high frequency smaller semicircle to charge-transfer at the cathode [18–20]. However, the impedance data of the $LiCoO_2$ electrode alone have been shown to contain two semicircles [21, 22] and it has been concluded that the formation of a surface layer on the $LiCoO_2$ was responsible for the high frequency smaller semicircle. In the present study also, as discussed later, the kinetic treatment suggests that the high frequency semicircle (Figure 2) is not due to an electrochemical process and is therefore attributed to the surface layer on the electrodes.

It is found that R_1 is nearly invariant with SOC, whereas there is a noticeable decrease in R_1 with an increase in temperature (Table 1). Since R_1 is attributed to the resistance of a surface passive layer on the electrodes, a decrease in its magnitude with temperature (T) suggests that the layer is ionically conducting [21]. Plots of $\ln(1/R_1)$ against $10^3/T$ (Figure 4) at all SOC values are found to be linear, and therefore the Arrhenius equation is considered to be valid:

$$\frac{1}{R_1} = A_o \exp\left(-\frac{E_a}{RT}\right) \tag{5}$$

where A_o is a constant and E_a the activation energy. The value of E_a calculated for several SOC values is in the range 0.35 to 0.45 eV.

There is a weak dependence of Q_1 on SOC as well as on T. At SOC ≈ 0.5, for instance, there is an increase in Q_1 from 0.521 at -10 °C to 0.959 at 40 °C (Table 1). An

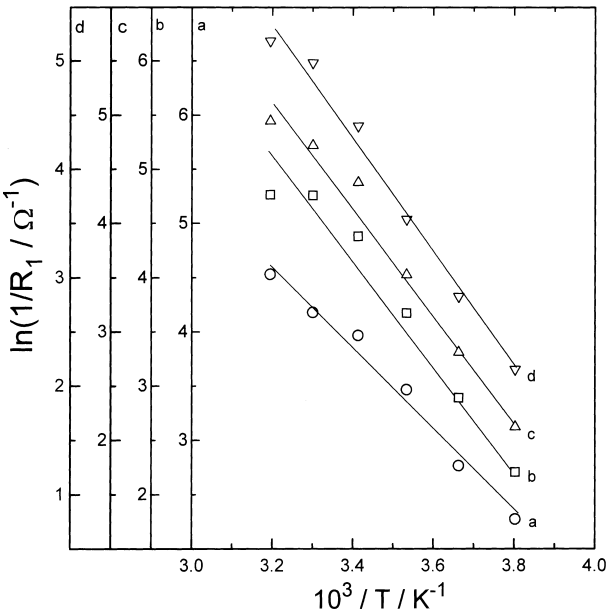

Fig. 4. Plots of ln $(1/R_1)$ against inverse of temperature (T) for SOC values (a) 1, (b) 0.8, (c) 0.5 and (d) 0.2. Different scales on ordinate (a–d), respectively, correspond to the curves (a)–(d).

increase in the value of n_1 to unity with increase in temperature suggests that the surface layer exhibits capacitance behaviour at high temperature.

There is a strong dependence of R_2 on the SOC (Figure 5) and also on temperature (Table 1). Since R_2 is attributed to the electrochemical reactions, it is considered as the charge-transfer resistance (R_{ct}) of the lithium-ion cell. Unlike R_2, the variation in the value of Q_2 is not substantial. Since the value of n_2 is close to unity (Table 1), Q_2 is approximated to double-layer capacitance (C_{dl}).

The impedance (Z) of the parallel combination of R_{ct} and C_{dl} in the frequency range of 100 Hz–10 mHz, that is, corresponding to the low frequency semicircle (Figure 2) is thus given by Equation 6:

$$Z = \frac{R_{ct}}{1 - \omega^2 C_{dl}^2 R_{ct}^2} + \frac{j\omega C_{dl} R_{ct}^2}{1 - \omega^2 C_{dl}^2 R_{ct}^2} \tag{6}$$

where $R_{ct}/(1 - \omega^2 C_{dl}^2 R_{ct}^2)$ forms the real component of the impedance (Z') and $\omega C_{dl} R_{ct}^2/(1 - \omega^2 C_{dl}^2 R_{ct}^2)$ the imaginary component (Z'').

The electron-transfer process of the electrodes of a Li-ion cell may be written in a general way as follows:

$$X + Li^+ + e^- \underset{\text{deintercalation}}{\overset{\text{intercalation}}{\rightleftharpoons}} Y \tag{7}$$

where X stands for $Li_{1-x}C$ and $Li_{1-x}CoO_2$ in Equations 1 and 2, respectively, and Y for LiC and $LiCoO_2$. The R_{ct} for Reaction 7 is related to the reaction kinetics from Butler–Volmer equation for charge-transfer controlled electrochemical reaction [23]:

$$R_{ct} = \frac{RT}{FI_o} \tag{8}$$

where I_o is the exchange current of the reaction. The values of I_o of the Li-ion cell are calculated, and its variation with SOC at a few temperatures is shown in Figure. 6. The value of I_o increases with SOC and also with temperature. For instance at 40 °C, there is an increase in I_o from about 350 mA at SOC $\approx$ 0.1 to about 650 mA at SOC $\approx$ 1; and at SOC $\approx$ 1, an increase from about 12 mA at −10 °C to about 650 mA at 40 °C is also evident (Figure 6). The poor

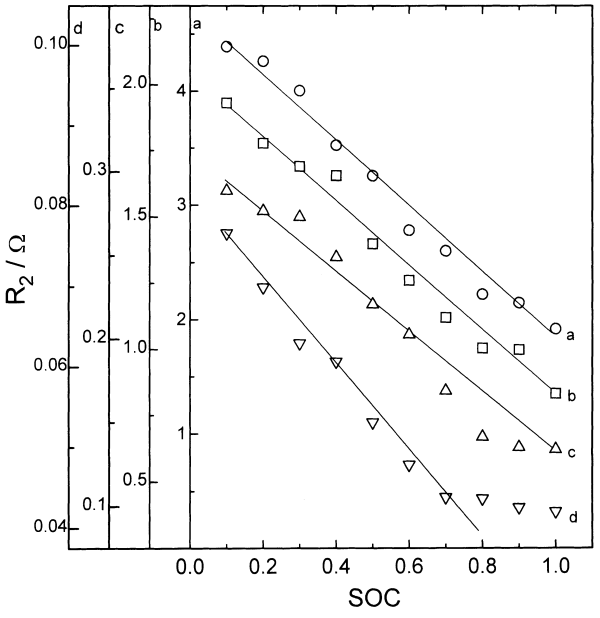

Fig. 5. The variation of resistance R_2 with SOC at temperature (a) −10, (b) 0, (c) 20 and (d) 40 °C. Different scales on ordinate (a–d), respectively, correspond to the curves (a)–(d).

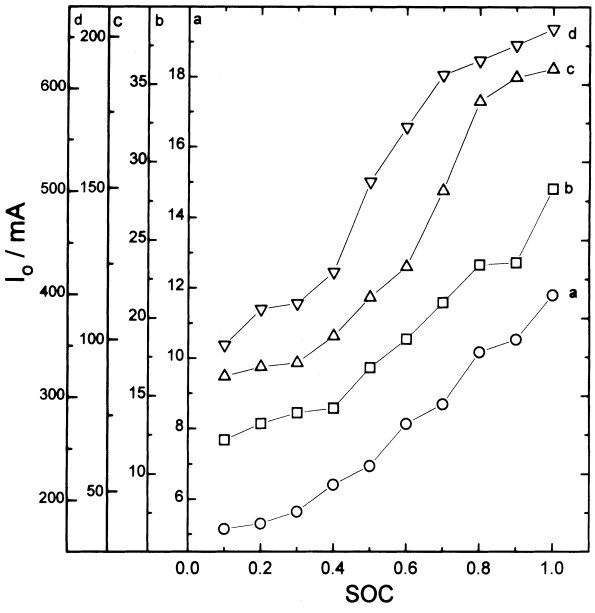

Fig. 6. Variation of exchange current (I_o) with SOC at temperature (a) −10. (b) 0, (c) 20 and (d) 40 °C. Different scales on ordinate (a–d), respectively, correspond to the curves (a)–(d).

discharge capacity of the Li-ion cell at sub-ambient temperatures (Figure 1), thus, is due to very low values of I_o.

The relationship between I_o and concentration (c) of Li^+ ions is as given in Equation 9.

$$I_o = FAk_s c^\alpha \tag{9}$$

where A is the electrode area, k_s the standard rate constant and α the transfer coefficient. The concentration of the Li^+ ions in the electrolyte is constant during the charge–discharge cycling process, which is reflected in the overall cell reaction (Equation 3). The discharge capacity of an electrode is governed by the amount of Li^+, which can undergo intercalation and deintercalation. In the case of $LiCoO_2$, for instance, the variation of composition is from $LiCoO_2$ at SOC $\approx$ 0 to $Li_{0.5}CoO_2$ at SOC $\approx$ 1. Thus the SOC may be defined as the ratio of the amount (c) of Li that is available for extraction to the maximum amount (c_s) that can be extracted from the electrode. Thus,

$$S = c/c_s \tag{10}$$

where SOC is abbreviated as S. Therefore,

$$c^\alpha = k_1 S^\alpha \tag{11}$$

where k_1 ($=c_S^\alpha$) is a constant.

From Equations 9 and 11, we can write Equation 8 as in Equation 12.

$$R_{ct} = \frac{RT}{F^2 A k_s k_1 S^\alpha} \tag{12}$$

The standard rate constant (k_s) depends on T, and the relationship follows the Arrhenius equation:

$$k_s = A_o \exp(-E_a/RT) \tag{13}$$

By substitution of k_s from Equation 13, Equation 12 becomes:

$$R_{ct} = \frac{RT \exp(E_a/RT)}{F^2 A k_1 A_o S^\alpha} \tag{14}$$

or

$$R_{ct} = \frac{kT \exp(E_a/RT)}{S^\alpha} \tag{15}$$

where k ($=1/(F^2 A k_1 A_o)$) is constant, which is independent of T and SOC. Since T and S are independent of each other, we can rewrite Equation 15 as in Equation 16.

$$\ln(R_{ct}/T) = \ln k + (E_a/(RT)) - \alpha \ln S \tag{16}$$

On differentiation, we obtain

$$\frac{d \ln(R_{ct}/T)}{d(1/T)} = \frac{E_a}{R} \tag{17}$$

and

$$\frac{d \ln(R_{ct}/T)}{d \ln S} = -\alpha \tag{18}$$

Thus, it is possible to evaluate apparent activation energy (E_a) and apparent transfer coefficient (α) of the Li-ion cell reaction.

The variations of ln (R_{ct}/T) with $10^3/T$, and ln (R_{ct}/T) with ln S of the Li-ion cell are shown in Figures 7 and 8, respectively. It is seen that the plots are linear as expected from Equations 17 and 18. The values of E_a obtained from Figure 7 for different SOC values are in the range 0.58–0.62 eV range; the α values are obtained from Figure 8 for different temperatures are in the range 0.38–0.42. It may be noted that the E_a of the lithium-ion cell reaction is nearly invariant with SOC. The values α are close to 0.5, what is expected for reversible electrochemical reactions.

Thus it is evident from the above discussion that the low frequency semicircle of the impedance spectrum (Figure 2) arises from the charge-transfer process of the Li-ion cell. A similar analysis was applied to the high frequency smaller semicircle in order to examine if this semicircle also was due to an electron transfer process. A plot of ln (R_1/T) versus ln S was nonlinear and an approximate linear fit of the data resulted in a value of <0.04 for α. This value of α is not expected for reversible electron transfer reaction of the Li-ion cell. Thus it is concluded that the high frequency semicircle does not correspond to the electrochemical reactions of either of the two electrodes, and the low frequency semicircle of

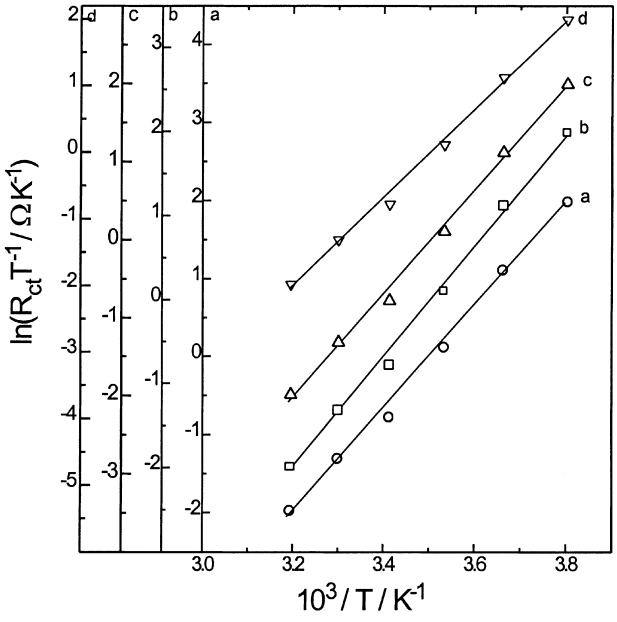

Fig. 7. Plots of ln (R_{ct}/T) against inverse of temperature (T) for SOC (a) 1, (b) 0.8, (c) 0.5 and (d) 0.2. Different scales on ordinate (a–d), respectively, correspond to the curves (a)–(d).

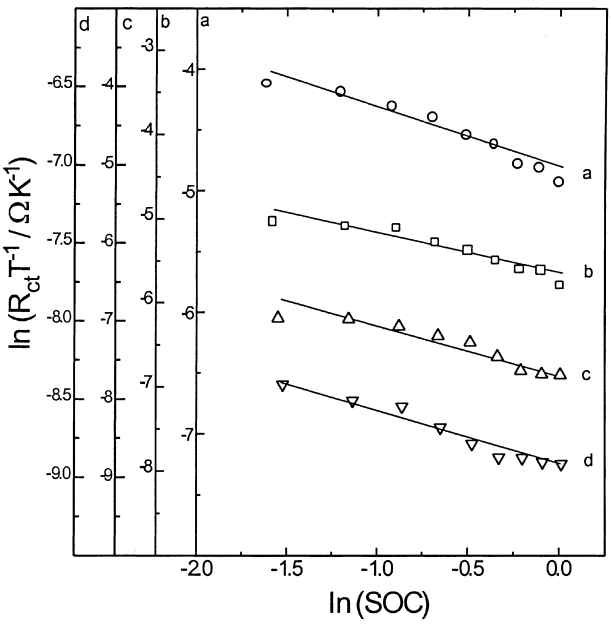

Fig. 8. Plots of ln (R_{ct}/T) against SOC at temperature (a) −10, (b) 0, (c) 20 and (d) 40 °C. Different scales on ordinate (a–d), respectively, correspond to the curves (a)–(d).

bigger size corresponds to the electrochemical reactions of the cell. As the kinetics of both the electrode reactions is similar, it is possible that the *RC* time constants of the anode and cathode processes are similar in magnitude, which results in a single semicircle.

4. Conclusions

A.c. impedance behaviour of a commercial sealed Li-ion cell is studied in the temperature range −10 and 40 °C for various state-of-charge (SOC) values. The resistance corresponding to the high frequency semicircle of the Nyquist impedance plot is attributed to the surface film on the electrodes as these data do not follow the kinetic relationship. The resistance corresponding to the low frequency semicircle is due to the electrode reactions, and it exhibits a strong dependence on the SOC and temperature. The data are analyzed using the Butler–Volmer kinetic equation for activation controlled charge-transfer reaction, and the kinetic parameters, namely, the apparent exchange current, transfer coefficient and activation energy of the cell reaction are evaluated. The poor discharge capacity of the Li-ion cell at subambient temperatures is due to very low values of exchange current of the cell reaction.

Acknowledgements

Authors thank the Ministry of Non-Conventional Energy Sources, Government of India for financial support.

References

1. J.R. Macdonald , 'Impedance Spectroscopy' (John Wiley & Sons, New York, 1987), p. 84.
2. S. Rodrigues, N. Munichandraiah and A.K. Shukla, *J. Power Sources* **87** (2000) 12.
3. F. Huet, *J. Power Sources* **70** (1998) 59.
4. N.A. Hampson, S.A.G.R. Karunathilaka and R. Leek, *J. Appl. Electrochem.* **10** (1980) 3.
5. T. Tanaka, K. Ohta and N. Arai, *J. Power Sources* **97–98** (2001) 2.
6. D. Linden 'Handbook of Batteries', McGraw Hill, New York (1995) p 14.1.
7. G. Pistoia, 'Lithium Batteries' (Elsevier, Amsterdam, 1994), p. 1.
8. G. Nagasubramanian, *J. Appl. Electrochem.* **31** (2001) 99.
9. H-P. Lin, D. Chua, M. Saloman, H-C. Shiao, M. Hendrickson, E. Plichta and S. Slane, *Electrochem. Solid-State Lett.* **4** (2001) A71.
10. H-C. (Alex) Shiao, D. Chua, H-P. Lin and S. Slane and M. Salomon, *J. Power Sources* **87** (2000) 167.
11. M.C. Smart, B.V. Ratnakumar, S. Surampudi, Y. Wang, X. Zhang, S.G. Greenbaum, A. Hightower, C.C. Ahn and B. Fultz, *J. Electrochem. Soc.* **146** (1999) 3963.
12. B.A. Boukamp, 'Equivalent Circuit, Users Manual' (University of Twente, The Netherlands, 1989), p. 1.
13. R. Greef, R. Peat, L.M. Peter, D. Pletcher and J. Robinson 'Instrumental Methods in Electrochemistry' (Ellis Horwood, Chichester, 1985), p. 263.
14. R.R. Bevington, 'Data Reduction and Error Analysis for the Physical Sciences' (McGraw-Hill, New York, 1969), p. 1.
15. S. Rodrigues, N. Munichandraiah and A.K. Shukla, *J. Solid State Electrochem.* **3** (1999) 397.
16. F. Gutmann, *J . Electrochem. Soc.* **112** (1965) 94.
17. M. Keddam, Z. Stoynov and H. Takenouti, *J. Appl. Electrochem.* **7** (1977) 539.
18. K. Ozawa, *Solid State Ionics* **69** (1998) 212.
19. M.J. Isaacson, M.E. Daman and R.P. Hollandsworth, *in* E.J. Cairns and F. McLarnan (Eds), 'Proceedings of the 32nd Intersociety Energy Conversion Engineering Conference', (American Institute of Chemical Engineers, New York, 1997), p. 31.
20. P.O. Braatz, K.C. Lim, A.M. Lackner, W.H. Smith, J.D. Margerum and H.S. Lim, *in* 'Abstracts of Joint International Meeting on Batteries and Fuel cells for Portable Applications and Electric Vehicles' (The Electrochemical Society, Pennington, NJ, 1997), p. 134.
21. M.G.S.R. Thomas, P.G. Bruce and J.B. Goodenough, *J. Electrochem. Soc.* **132** (1985) 1521.
22. D. Aurbach, M.D. Levi, E. Levi and A. Schechter, *in* Abstracts of Joint International Meeting on 'Batteries and Fuel cells for Portable Applications and Electric Vehicles' (The Electrochemical Society, Pennington, NJ, 1997), p. 124.
23. A.J. Bard and L.R. Faulkner, *in* 'Electrochemical Methods' (J. Wiley & Sons, New York, 1980), p. 105.